metals

MDPI

Article

Effect of Repeated Processing Passes during Ultrasonic Rolling on Fatigue Performance and Corrosion Resistance of Ti6Al4V Alloy

Shuaixing Wang [1,2,*], Tianjian Yu [2], Zhiwei Pang [2], Xiaole Yin [2] and Xiaohui Liu [1,2]

[1] National Defense Key Discipline Laboratory of Light Alloy Processing Science and Technology, Nanchang Hangkong University, Nanchang 330063, China; 71257@nchu.edu.cn
[2] School of Materials Science and Engineering, Nanchang Hangkong University, Nanchang 330063, China; 2101085600015@stu.nchu.edu.cn (T.Y.); jesspang@163.com (Z.P.); yinxiaole_8@163.com (X.Y.)
* Correspondence: wangsx@nchu.edu.cn

Abstract: Ultrasonic surface rolling processing (USRP) is a new method to improve the fatigue performance of titanium alloy, and repeated processing pass is an important factor that affects its strengthening effect. The effect of USRP passes on the surface microstructure, residual stress, fatigue performance and corrosion resistance of titanium alloy is researched via SEM, X-ray diffractometer, rotating–bending fatigue test and electrochemical impedance spectroscopy. The results show that Ti6Al4V alloy undergoes cumulative plastic deformation during USRP process, the surface grains are refined and a residual compressive stress field with a thickness of 500 μm is introduced, which together improve the fatigue performance of the Ti6Al4V alloy. Increasing the repeated processing passes will deepen the grain refinement layer and increase the surface hardening effect, but the fatigue life of the Ti6Al4V alloy does not increase with an increase in processing passes. A five-passes processing under a static force of 550 N can result in a greater gain for the fatigue resistance of the Ti6Al4V alloy; the fatigue life of a five-passes-processed sample under 600 MPa is 8 times higher than that of an untreated sample, and its fatigue crack source initiates at the subsurface away from the surface of 180 μm. Furthermore, Ti6Al4V alloys treated by USRP show a better corrosion resistance in both neutral and acidic solutions, especially for the five-passes-processed sample.

Keywords: corrosion resistance; fatigue performance; residual compressive stress; Ti6Al4V alloy; ultrasonic rolling processing passes

check for updates

Citation: Wang, S.; Yu, T.; Pang, Z.; Yin, X.; Liu, X. Effect of Repeated Processing Passes during Ultrasonic Rolling on Fatigue Performance and Corrosion Resistance of Ti6Al4V Alloy. *Metals* **2023**, *13*, 1719. https://doi.org/10.3390/met13101719

Academic Editor: Zbigniew Pater

Received: 14 September 2023
Revised: 3 October 2023
Accepted: 5 October 2023
Published: 9 October 2023

Copyright: © 2023 by the authors. Licensee MDPI, Basel, Switzerland. This article is an open access article distributed under the terms and conditions of the Creative Commons Attribution (CC BY) license (https://creativecommons.org/licenses/by/4.0/).

1. Introduction

Titanium and titanium alloys are widely used in the production of aviation components due to their low density, high specific strength and good corrosion resistance [1–3]. However, titanium alloys also have the disadvantages of poor wear resistance and high notch sensitivity. Surface deformation-strengthening techniques, such as shot peening (SP), deep rolling (DR), ultrasonic impact treatment (UIT), laser shock peening (LSP) and ultrasonic surface rolling processing (USRP), have been recognized as effective means to overcome the above mentioned shortcomings of titanium alloys [4–10]. Although these treatments can provide some improvements in the fatigue performance of titanium alloys, different techniques have their own characteristics and application scopes. In contrast, the USRP technique combines the effects of ultrasonic frequency vibration and static machining, so it may offer better surface integrity and superior results for titanium alloy parts [9–14].

In recent years, the ultrasonic rolling of titanium alloys has gradually attracted attention. Several studies suggest that static force has a greater impact on the surface integrity of TC17 alloy compared with feed rate [12]. Static load and spindle speed are also the important parameters to determine the deformation degree of the Ti6Al4V alloy [14,15]. The

smaller static force in ultrasonic rolling processing can generate uniform plastic deformation on the surface of the Ti6Al4V alloy and significantly improve its microhardness [14,16]. A spindle speed of 200 rpm can achieve a higher surface integrity and optimal fatigue resistance for the Ti6Al4V alloy [15]. Furthermore, it has been proven that processing passes have the greatest impact on the residual stress field [11,17]. Liu et al. determined that a compressive stress field with a thickness of 530 μm was formed and the fretting fatigue limit of the Ti6Al4V alloy was optimal after single-pass treatment with USRP [11,18]. But, on the other hand, Li et al., found that the high-cycle fatigue performance of the Ti6Al4V alloy can only be greatly improved after the multi-pass processing of USRP [17]. In general, ultrasonic rolling process conditions are closely related to the factors that determine the fatigue performance (surface roughness, hardness, residual stress distribution, etc.), but there is no unified understanding on the influence laws of ultrasonic rolling parameters. Therefore, the ultrasonic rolling process conditions, especially the processing passes, can be further optimized in order to obtain a better anti-fatigue effect.

In addition, surface strengthening may also cause changes in the electrochemical properties of materials due to the severe deformation and refinement of the surface structure. Several studies have shown that surface strengthening reduces the corrosion performance of materials [19–22]. The nanostructure of cp-Ti leads to a decrease in corrosion resistance in a 0.9% NaCl solution compared with coarse-grained material [20]. The corrosion rate of nanostructured surface layers prepared via shot peening on 6061 and 7075 aluminum alloys is significantly higher than that of the bulk material [21]. However, some research works confirmed that ultrasonic rolling treatment can significantly improve the pitting corrosion resistance of 7B50 aluminum alloy and Z5CND16-4 martensitic stainless steel [22,23]. Furthermore, the gradient nanostructures formed on pure Ti treated by ultrasonic rolling caused its corrosion current density and passivation current density to decrease by 70% and 54%, respectively [24]. The hot corrosion rate of the ultrasonic shot-peened samples is also lower compared to the untreated Ti6Al4V alloy [25]. There is considerable disagreement among these studies on the effect of surface strengthening on the corrosion behavior of materials. Therefore, it is necessary to study the effect of ultrasonic rolling treatment on the corrosion resistance of the Ti6Al4V alloy.

In short, the repeated processing pass is an important parameter affecting the USRP strengthening effect, but the current research on its effect on surface structure and performance of titanium alloys is not systematic; the effect on corrosion resistance is especially rarely reported. Thus, researching the effects of ultrasonic rolling processing passes on the surface morphology, microhardness and residual stress of the Ti6Al4V alloy, as well as analyzing the fatigue and corrosion resistance of titanium alloys under different states, play positive roles in optimizing the ultrasonic rolling technique and improving the fatigue performance of titanium alloys.

2. Experimental Section

2.1. Materials

Ti6Al4V alloy bars with the diameter of φ 13 produced by Baotai Co. Ltd., Baoji, China are used in this work, whose main chemical composition (wt. %) is 6.70 Al, 4.20 V, 0.30 Fe, 0.03 C, 0.15 N, 0.14 O and balance Ti. The bars are formed by hot rolling, which are vacuum-annealed at 890 °C for 1 h and then cooled to room temperature before use. As shown in Figure 1a, Ti6Al4V alloy mainly has the typical primary structure of α + β and the secondary α phase. Furthermore, Figure 1b presents the geometric dimensions of the sample for USRP and fatigue test.

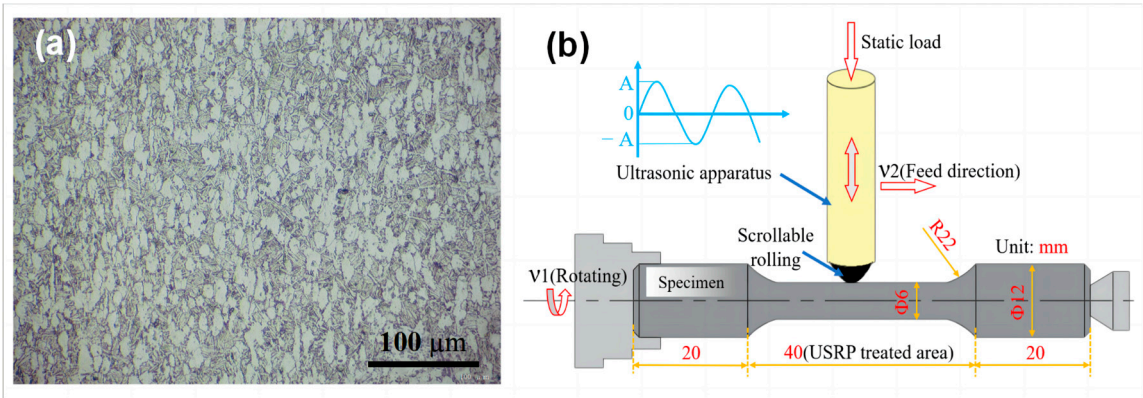


Figure 1. The metallographic structure of Ti6Al4V alloy (**a**) and the geometric dimensions of fatigue sample and schematic of ultrasonic rolling processing device (**b**).

2.2. USRP Treatment

USRP treatment of Ti6Al4V alloy is carried out using an ultrasonic rolling processing device (HK30G, Shandong Huawin Electrical and Mechanical Technology Co., Ltd., Jinan, China), as schematically illustrated in Figure 1b, and the specific details can also be found in refs. [11] and [18]. A smooth (Ra ≈ 0.1 μm) and scrollable WC/Co ball with a diameter of 14 mm rolls and hits the sample surface to perform plastic processing. The ultrasonic vibration frequency, vibration amplitude, static force, feeding rate and spindle speed are 27 kHz, 5 μm, 550 N, 0.20 mm and 100 rpm, respectively. While keeping the above parameters unchanged, the repeated processing passes are adjusted between 1 and 20 to treat the sample.

2.3. Microstructure Characterization

The surface and cross-sectional microstructure of Ti6Al4V alloy samples are observed via KH-7700 three-dimensional microscope (Hirox Co., Ltd., Tokyo, Japan) and FESEM (Nova Nano SEM450, FEI Co., Ltd., USA), respectively. The surface roughness (R_a) of different samples are measured using JB-6C profilometer. The microhardness of different samples are measured via Q10A+ Vickers hardness tester (Quness Co., Ltd., Salzburg, Austria) under a load of 0.25 N for 15 s. Furthermore, the residual stress for the samples is measured using an X-ray diffractometer (Proto-LXRD, Proto Manufacturing Ltd., LaSalle, ON, Canada) with Cu-Kα radiation. The tube voltage and current are 30 kV and 20mA, respectively. When testing the depth distribution of residual stress, Ti6Al4V alloy is removed using an electrolytic polishing machine (Proto-8818, Proto Manufacturing Ltd., LaSalle, ON, Canada) in saturated NaCl solution at 1 V.

2.4. Fatigue Test and Electrochemical Test

Fatigue tests of Ti6Al4V alloy samples are conducted by a PQ-6 rotary bending fatigue tester (Ningxia Qing Shan Testing Machine Co. Ltd, Yinchuan, China) in air at room temperature. The four-point force method is used to test with a frequency of 50 Hz and stress ratio of −1. Based on the tensile strength (900~1000 MPa) and fatigue limit (~500 MPa) of Ti6Al4V alloy [18,26], 700 MPa and 600 MPa are selected to compare the fatigue performance of Ti6Al4V alloy before and after USRP. At least three samples shall be tested under each condition to ensure the reliability of data. The fracture morphology after fatigue test is observed via SEM (SU 1510, Hitachi Co., Tokyo, Japan).

Electrochemical impedance spectroscopy (EIS) is conducted using an CHI604D electrochemical workstation (Shanghai Chenhua Instrument Co., Ltd, Shanghai, China). The reference and counter electrodes are saturated calomel electrode (SCE) and platinum plate, respectively. The working electrode is a Ti6Al4V sample inlaid in epoxy resin with an effective area of 1 cm^2. EIS are acquired at open circuit potential (OCP) over the frequency

range of 10^{-2}~10^{5} Hz using an AC signal amplitude of 10 mV. All tests are performed at 25 °C and repeated in three samples to ensure the reliability of results.

3. Results and Discussion

3.1. Surface Morphology of Ti6Al4V Alloy in Different Processing States

Figure 2 shows the surface morphology of a Ti6Al4V alloy with different states. As shown in Figure 2a,b, the surface of the untreated sample has approximately periodic machining traces along the chip direction and a few deep pits, resulting in the higher R_a value of 0.317 µm. After USRP treatment, the surface flatness of the Ti6Al4V alloy samples is significantly improved; the surface machining traces are basically eliminated, so R_a value is greatly reduced, as shown in Figure 2c–l. By comparison, it can be found that there remains small cracks and pits on the surface of the single-pass-processed sample; the surface state of the samples are more uniform when the processing passes increase to 5~10, but the surface reappears with pits, and the surface roughness increases if excessive processing passes (15~20) are executed.

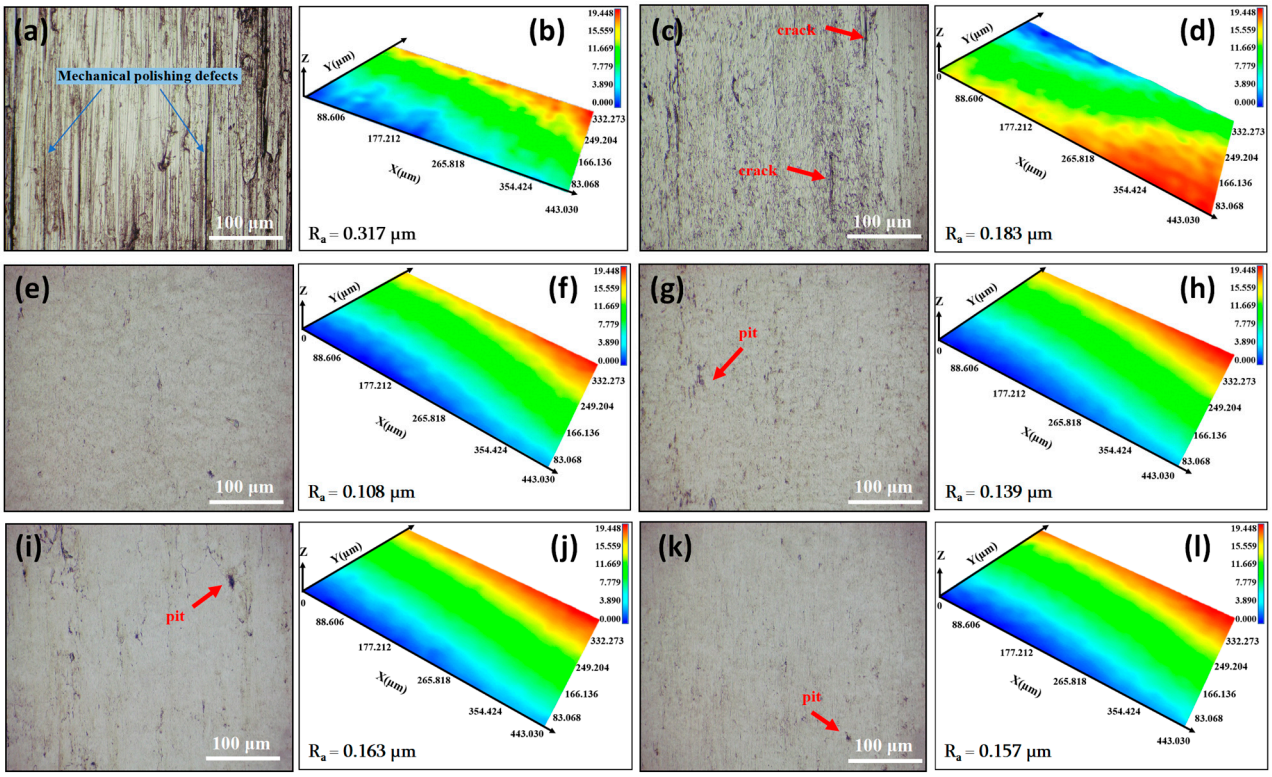


Figure 2. OM (**a**,**c**,**e**,**g**,**i**,**k**) and 3D images (**b**,**d**,**f**,**h**,**j**,**l**) of surface morphology for untreated Ti6Al4V alloy (**a**,**b**) and treated by USRP of 1 pass (**c**,**d**), 5 passes (**e**,**f**), 10 passes (**g**,**h**), 15 passes (**i**,**j**) and 20 passes (**k**,**l**).

As is well known, ultrasonic rolling performs plastic processing on the metal surface via the combination of ultrasonic impact and static rolling [9–18]. During an ultrasonic rolling process, high-frequency ultrasonic waves applied on the sample surface make the atoms inside the material constantly oscillate, while the hard ball always rolls and hits the sample surface at a high speed under static force, these combined action makes the oscillating atoms migrate in the same direction and so produces the plastic deformation on the metal surface [12,15,17,18]. The cumulative processing effect flattens the protrusions on the sample surface and flows into the pits or valleys, thereby achieving a smoothing effect. Meanwhile, the plastic deformation causes the dislocations to move and intersect, resulting in the refinement of grains and the significant reduction in roughness [13,27,28]. The force acting on the sample surface during single-pass processing is limited; some deep

machining traces cannot be completely filled, so the roughness is high at this time. The processing coverage on the sample surface will increase if the repeated processing passes are increased, whereby more macroscopic defects are eliminated, so the surface roughness significantly decreases. However, excessive processing passes will result in the superfluous work hardening of the surface layer and reduce its plasticity, which causes cracks to easily form on the sample surface, as well as pits and other defects, during processing, thus negatively affecting the surface quality.

3.2. Microstructure and Stress Distribution of Ti6Al4V Alloy with Different States

Figure 3 shows the cross-section morphology of Ti6Al4V samples treated by USRP with different processing passes. Ti6Al4V alloy undergoes obvious plastic deformation to form a gradient-strengthening layer after USRP treatment. The surface grains are obviously refined and deflected at a certain angle, but the grain size gradually increases with increasing depth. The thickness of the deformation layer and the deflection angle of grains successively increase as the processing passes increase, and the degree of grain refinement is also more obvious. As shown in Figure 3a, the thickness of the plastic deformation layer for a single-pass-processed sample is only 16 μm, and the deflection angle of grains is about 5.2°. When the repeated processing passes increase to twenty, the thickness of the gradient deformation layer reaches 230 μm, and the deflection angle of grains also increases to 37.8°, as shown in Figure 3d. Furthermore, the surface work hardening effect is more significant and the microhardness gradually increases with the increase in processing passes. The surface hardness of the single-pass-processed sample is almost equal to that of the Ti6Al4V alloy matrix (~330 HV), but the surface hardness of a twenty-passes-processed sample increases to 385 HV.

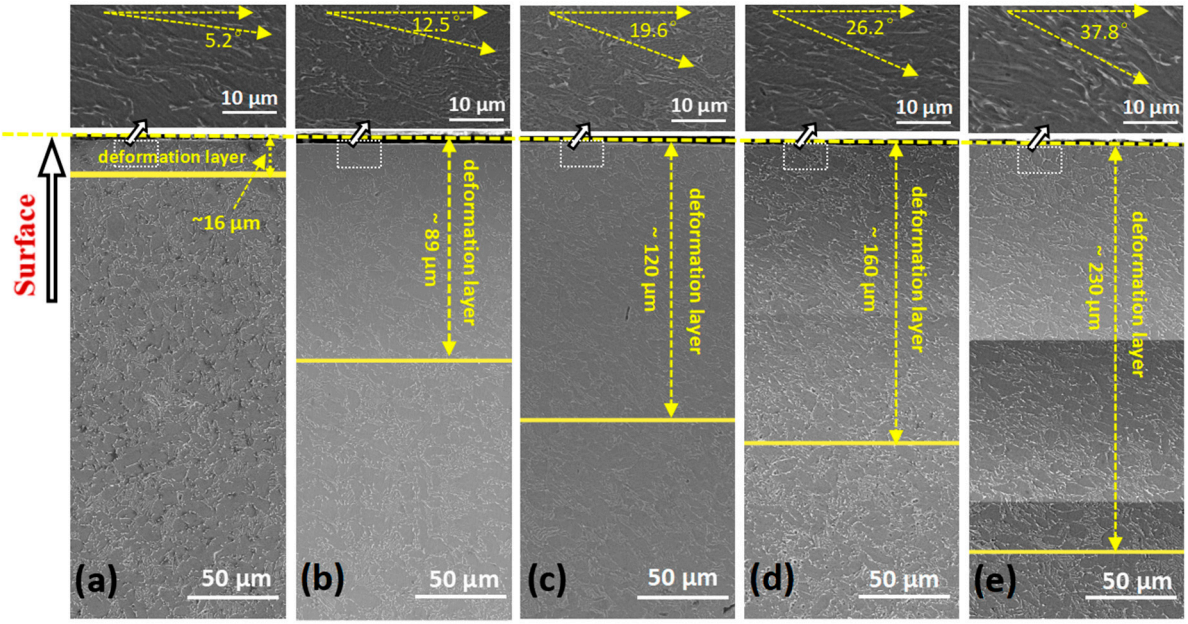


Figure 3. Cross-section microstructure of Ti6Al4V samples treated by USRP of 1 pass (**a**), 5 passes (**b**), 10 passes (**c**), 15 passes (**d**) and 20 passes (**e**).

Figure 4 shows the residual stress curves of Ti6Al4V alloy with different states. A gradient residual compressive stress field is introduced on the surface of Ti6Al4V alloy after USRP treatment. The maximum value and attenuation amplitude of residual stress for Ti6Al4V samples are different after conducting different processing passes of USRP. The residual stress value of the single-pass-processed sample is the largest at the surface (−609 MPa), and then it decreases rapidly along the depth direction, and is about −301 MPa when 200 μm away from the surface. Both the maximum stress values of the samples treated with five passes and twenty passes are at 30 μm away from the surface and are relatively

close in value (~600 MPa). However, the residual stress value of five-passes-processed sample decreased significantly slower, and is still −390 MPa at a distance of 500 μm from the surface, which is significantly larger than that of other samples.

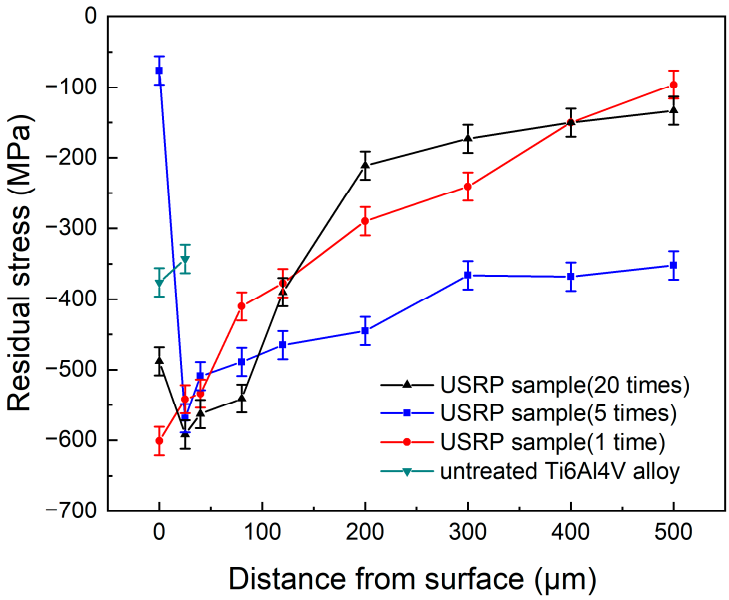


Figure 4. Residual stress curves of Ti6Al4V alloy with different processing states.

Various research studies have confirmed that the dislocations inside the original coarse grains of titanium alloy may slip, interlace, entangle and rearrange as the high-frequency impact energy and static force during the USRP process, and so the grains will be squashed, elongated and even broken [13,15,27–29]. After long-term pressure is applied, the surface grains of the material are gradually refined and the strain gradually aggravates to result in severe plastic deformation. Grain refinement increases the deformation resistance of grain boundaries. The intersection and multiplication of dislocations also increase the work hardening effect, which together improve the surface hardness of the sample [8,11,17,30,31]. The accumulated plastic deformation on the sample surface will form an equilibrium constraint with the inner undeformed area, resulting in a large residual compressive stress on its surface. Furthermore, the sample will be simultaneously subjected to the perpendicular pressure and tangential shear force during USRP, which makes the grains deflect at a certain angle. Different processing passes lead to different degrees of plastic deformation, thereby affecting the stress distribution and microhardness. When there are fewer processing passes, the plastic deformation is limited due to less energy injection, so only a low residual compressive stress is introduced. By increasing the number of repeated processing passes, the frequency of ultrasonic impact and rolling force that is applied on the sample increases. The grains are more likely to be compressed and rearranged, so the plastic deformation degree significantly enhances and the surface microhardness also shows an increasing trend. However, excessive processing passes will make the steady-state atoms re-oscillate and cause local elastic deformation; and so, the residual compressive stress presents a larger fluctuation. Therefore, a proper processing pass is the key to ensure reasonable plastic deformation and introduce effective residual compressive stress.

3.3. Fatigue Performance of Ti6Al4V Alloy with Different States

Figure 5 shows the fatigue life of the Ti6Al4V alloy under different states at 700 MPa and 600 MPa. The fatigue life of the Ti6Al4V alloy has been greatly improved by USRP treatment, but the fatigue life of different samples varies greatly with the processing passes. At 700 MPa, the fatigue life of the untreated sample is about 25 kilocycles; it has been increased by about 3 times after single-pass processing, but has little change if the processing passes continue to increase. At 600MPa, the fatigue life of the Ti6Al4V alloy is

more significantly increased by USRP treatment. After a single and five passes of USRP, the fatigue life of the samples reached 202 kilocycle and 329 kilocycles, respectively, which are nearly 5 times and 8 times higher than that of the untreated sample. However, the fatigue life of the Ti6Al4V sample actually decreases when the repeated processing passes reaches twenty. Overall, ultrasonic rolling processing can effectively improve the fatigue resistance of the Ti6Al4V alloy, and the anti-fatigue effect reaches a good state only when five passes are selected, especially in the high-cycle fatigue tests.

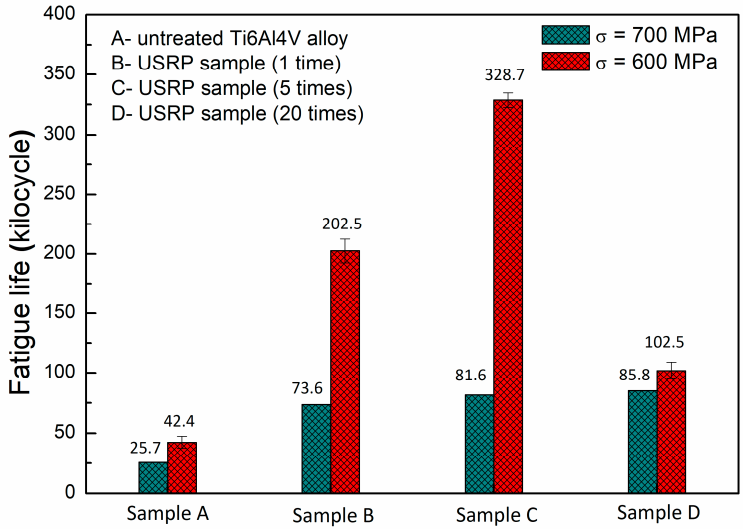


Figure 5. Fatigue life of Ti6Al4V alloy under different states at 700 MPa and 600 MPa.

Figure 6 presents the fracture morphology of different samples after a fatigue test at 600 MPa. As shown in Figure 6a–c, fatigue cracks of the untreated sample occur on the surface, then rapidly propagate along a fan-shaped path to the interior of the sample, and finally converge in region III to cause ductile fracture. The initiation and propagation of fatigue cracks for ultrasonic rolled samples have partially changed, which is related to the processing passes. For the samples treated by USRP of single pass and twenty passes, the crack source is still on the surface, but the crack source area is obviously flatter and smaller, as shown in Figure 6e,k. However, the crack source of the five-passes-processed sample transfers inward to the subsurface, away from the surface, by about 180 μm, as shown in Figure 6h. The crack initiates from the inside and expands radially to the surrounding area, and the area of the crack propagation zone is significantly larger.

It is generally believed that the fatigue life of materials mainly consists of crack initiation life and crack propagation life, the surface integrity and surface hardening layer will affect the initiation of cracks, while the residual compressive stress is closely related to the growth of cracks [7,11,15,32–35]. The surface of the untreated sample has obvious machining traces, pits and other defects (Figure 2a), which can easily cause stress concentration and become fatigue crack sources under alternating loads [7,15,17,18,32,34]. After USRP treatment, the surface roughness of the Ti6Al4V alloy decreases, the surface hardness increases and a grain refinement layer forms simultaneously (Figure 3). The improvement of surface integrity and the existence of a hardening layer help to hinder the formation of cracks, thus increasing the crack initiation life [17,18,33,34,36]. Meanwhile, a compressive stress field with a thickness of 500 μm is introduced into the sample surface under cumulative plastic deformation during USRP process (Figure 4), which offsets the effect of alternating stress to some extent and has a positive contribution to fatigue life. The surface roughness, hardening layer thickness and residual compressive stress of the Ti6AlV alloy will be significantly different if the USRP processing pass is changed, resulting in different initiation and propagation rules for the fatigue cracks.

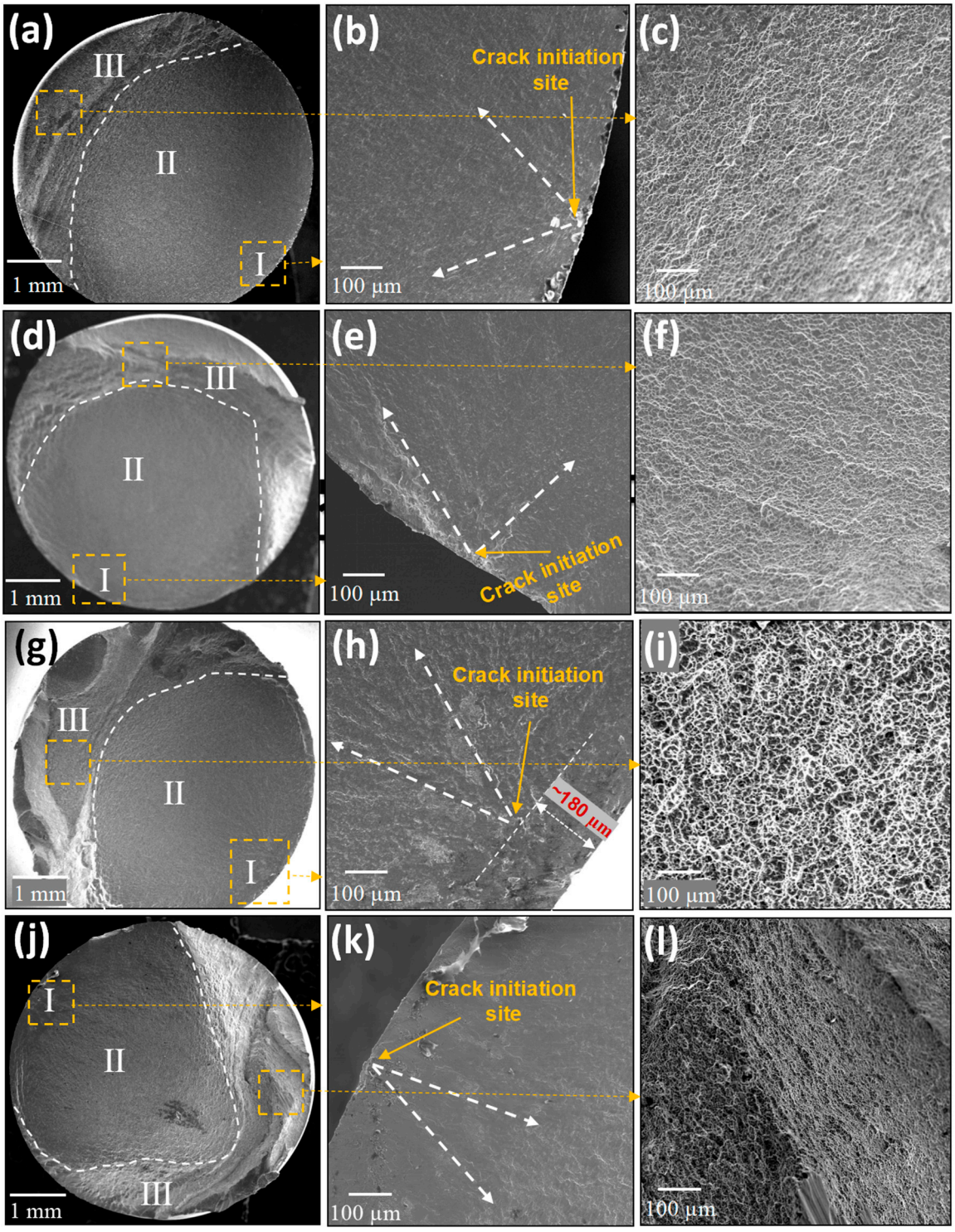


Figure 6. Fatigue fracture macroscopic morphology (**a**,**d**,**g**,**h**), enlarged image of crack initiation zone (**b**,**e**,**h**,**k**) and instantaneous fracture zone (**c**,**f**,**i**,**l**) of untreated Ti6Al4V alloy (**a**,**b**,**c**) and the samples treated by USRP of 1 pass (**d**,**e**,**f**), 5 passes (**g**,**h**,**i**) and 20 passes (**j**,**k**,**l**) after fatigue test at 600 MPa (I represents the crack initiation zone, II represents the crack propagation zone, and III represents the instantaneous fracture zone).

If the Ti6Al4V sample is subjected to single-pass processing, the surface roughness is still relatively high (Figure 2c) and the grain refinement layer is only 16 μm (Figure 3a), fatigue cracks are still prone to emerging at the surface defects (such as pits, micro-cracks), thus providing a lower gain in fatigue life. Although the plastic deformation layer is

deepened for the sample treated with 20 passes, the surface integrity deteriorates and the local stress relaxes due to excessive processing, the residual stress decreases rapidly along the depth direction and the stress value is only −205 MPa at a distance of 200 μm from the surface (Figure 4), which causes the fatigue crack source to still occur at the surface and rapidly expand [7,17,18,32]. Appropriate processing times can simultaneously ensure good surface integrity, grain refinement effect and introduce a deep and stable residual compressive stress field for titanium alloys. As shown in Figures 2e, 3b and 4, the surface roughness of the five-passes-processed sample is only 0.108 μm, and its residual stress value can still reach -390 MPa at a distance of 500 μm away from the surface. In contrast, the lower surface roughness reduces the stress concentration and hinders the crack initiation, and the deeper and stale compressive stress field effectively inhibits the propagation of fatigue cracks. The combined effect of these factors causes the five-passes-processed sample to exhibit a better fatigue resistance.

3.4. Electrochemical Corrosion Behavior of Ti6Al4V Samples with Different States

Figure 7 shows the electrochemical impedance spectra of the Ti6Al4V alloy with different states in 3.5 wt% NaCl and 1mol/L HCl solutions, respectively. As shown in Figure 7a, both untreated and ultrasonic rolled samples exhibit the characteristics of a double capacitive arc, but there are some differences in the high-frequency capacitive arc for the samples with different states. Generally, the low-frequency region of impedance spectra reflects the corrosion control steps, and the high-frequency loop represents the information of porous film on the electrode surface [37–40]. The impedance spectra can be fitted by the equivalent circuit shown in Figure 8, where R_s is the solution resistance; R_{ct} and Q_{dl} represent the charge transfer resistance and capacitance of the electric double layer at the metal–solution interface, respectively; R_f and Q_f correspond to the resistance and non-ideal capacitance of passivation film, respectively. Furthermore, Q is a constant phase element representing the dispersion effect of capacitance, and its value can be calculated using Equation (1) [37–39], where Y_0 is the admittance constant, and n is the frequency dispersion factor that varies from 1 to 0:

$$Q = {Y_0}^{-1}/(j\omega)^{n} \quad (1)$$

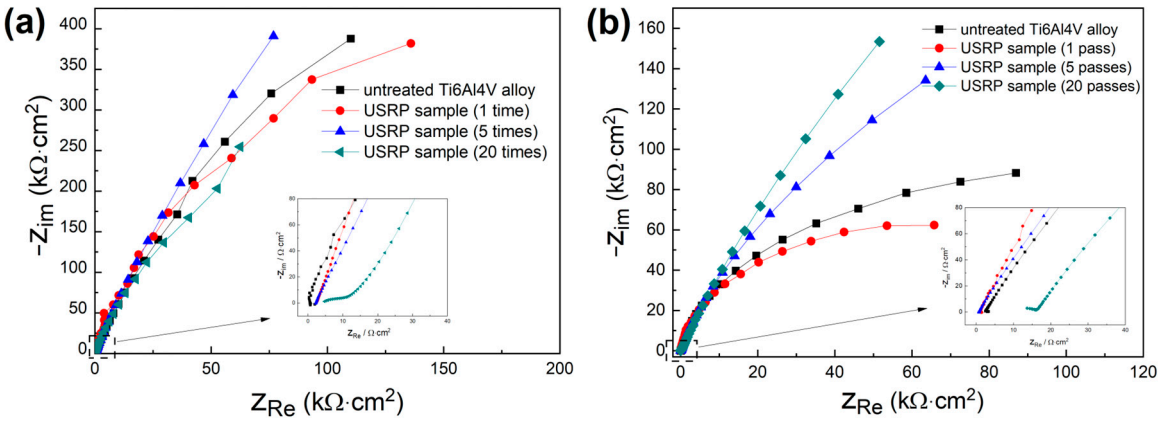


Figure 7. Nyquist diagrams of Ti6Al4V sample with different states in 3.5 wt% NaCl (**a**) and 1 mol/L HCl (**b**).

Table 1 shows the fitting values for the EIS of different samples in 3.5% NaCl solution. It can be found that the R_{ct} values of titanium alloy samples in different states are relatively close on the whole. Generally, R_{ct} is taken as a parameter to characterize the corrosion rate [38,39]. The similar values indicate that different samples have little difference in the corrosion resistance. However, from the perspective of R_f and Q_f, the coverage and compactness of the passivation film for ultrasonic rolled samples are improved, as evidenced

by the higher value of n_f [38–41]. Furthermore, the n_f value of the five-passes-processed sample is larger compared with other samples, indicating that its passivation film is denser and the corrosion resistance is slightly better.

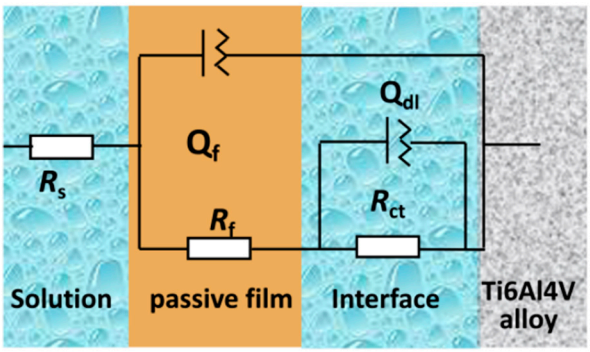


Figure 8. Equivalent circuit for EIS of Ti6Al4V samples in 3.5wt% NaCl and 1 mol/L HCl solution.

Table 1. Fitting results of EIS for Ti6Al4V samples with different states in 3.5% NaCl solution.

Ti6Al4V Samples	Q_f/F·cm^{-2}	n_f	R_f/Ω·cm^2	Q_{dl}/F·cm^{-2}	n_{dl}	R_{ct}/Ω·cm^2
untreated alloy	1.187×10^{-5}	0.901	288.6	1.756×10^{-5}	0.822	2.272×10^{6}
USRP sample (1 pass)	1.787×10^{-5}	0.927	356.7	7.859×10^{-6}	0.921	2.827×10^{6}
USRP sample (5 passes)	1.998×10^{-5}	0.939	362.4	1.036×10^{-5}	0.835	3.720×10^{6}
USRP sample (20 passes)	6.493×10^{-5}	0.916	420.4	4.01×10^{-5}	0.901	3.593×10^{6}

As shown in Figure 7b, the impedance spectra of all samples in acidic solution still show two capacitive arcs, but their impedance value are significantly smaller than that in a neutral system, showing that the corrosion resistance of the Ti6Al4V alloy in an acidic solution deteriorates. The equivalent circuit in Figure 8 is selected for fitting and the results are shown in Table 2. As shown in Figure 7b and Table 2, the R_{ct} value of ultrasonic-rolled samples is significantly higher than that of the untreated sample, indicating that ultrasonic rolling processing increases the corrosion reaction resistance of titanium alloys in acidic solutions. In addition, the comparison shows that the R_f value of a five-passes-processed sample is larger, and the n_f value is closer to 1, indicating that the thickness and density of the passivation film are significantly higher, the self-healing ability is stronger and the corrosion resistance is better [37,38,41].

Table 2. Fitting results of EIS for Ti6Al4V samples with different states in 1mol/L HCl solution.

Ti6Al4V Samples	Q_f/F·cm^{-2}	n_f	R_f/Ω·cm^2	Q_{dl}/F·cm^{-2}	n_{dl}	R_{ct}/Ω·cm^2
untreated alloy	5.018×10^{-5}	0.907	315.6	1.417×10^{-5}	0.9213	4.991×10^{4}
USRP sample (1 time)	6.726×10^{-5}	0.944	128.5	3.049×10^{-4}	0.8753	6.378×10^{4}
USRP sample (5 times)	1.788×10^{-5}	0.965	468.6	4.828×10^{-5}	0.8241	8.545×10^{5}
USRP sample (20 times)	2.842×10^{-5}	0.959	435.7	8.148×10^{-5}	0.6733	6.072×10^{4}

The analysis shows that titanium alloy undergoes cumulative plastic deformation during USRP; the surface grains are refined to form a gradient-strengthening layer under the combined action of high-frequency impact and rolling force, as shown in Figure 3. The refinement of grains shortens the distance between atoms, and the number of atoms per unit volume increases, so that the passivation film is easier to form and is more dense; the migration resistance of the corrosive media increases, improving the corrosion resistance [42–44]. On the contrary, the untreated sample has coarse grains and an uneven surface (Figure 2a), the passivation film is slightly less dense and uneven, so Cl^- ions easily penetrate the passivation film and cause a local corrosion of the sample [37,38].

However, the degree of surface grain refinement and surface integrity of the samples vary with ultrasonic rolling processing passes. If single-pass processing is selected, the grain refinement of titanium alloy is not enough, and the improvement of the corrosion resistance is relatively small. When Ti6Al4V alloy is treated for five passes, the surface grains are obviously refined and surface integrity is better, and the continuity of the passivation film may also be higher, resulting in a better corrosion resistance. Excessive processing will cause cracks or pits on the surface of the sample (Figure 2i,k); the continuity and uniformity of the surface structure is destroyed, which causes its passive current density and corrosion resistance to fluctuate within a certain range [41–45]. Overall, the corrosion resistance of Ti6Al4V samples with different processing states in neutral 3.5% NaCl solution is relatively close, but the ultrasonic rolled samples show a better passivation performance and corrosion resistance in 1 mol/L HCl solution, and the five-passes-processed samples are relatively better.

4. Conclusions

1. Ultrasonic rolling processing can cause cumulative plastic deformation on the surface of a Ti6Al4V alloy, refine the surface grains, and introduce residual compressive stress. Increasing the processing passes will deepen the grain refinement layer and significantly improve the surface hardness of the Ti6Al4V alloy. The depth of the plastic deformation layer for Ti6Al4V alloy can reach 230 μm after twenty passes of ultrasonic rolling, but excessive processing passes will adversely affect the surface integrity and cause the stress relaxation. Five passes of processing can introduce a more stable residual stress field, which can still reach a stress value of −390 MPa at a depth of 500 μm.
2. Ultrasonic rolling processing can effectively improve the fatigue resistance of Ti6Al4V alloy, but its fatigue life does not increase with the increase in processing passes. The anti-fatigue effect of the Ti6Al4V alloy reaches a better state when only five passes are selected. Under 600 MPa, the fatigue life of the Ti6Al4V alloy treated by USRP with five passes can reach 329 kilocycles, which is 8 times higher than that of the untreated sample. The lower surface roughness, suitable fine-grained strengthening layer, deep and stable residual compressive stress field together allows for the five-passes processing to provide greater gain for the fatigue resistance of the Ti6Al4V alloy.
3. Ultrasonic rolling processing can also endow the Ti6Al4V alloy with a better passive performance and improve its corrosion resistance to a certain extent, especially in an acidic solution system. Relatively speaking, the five-passes-processed samples performed better, which has a higher charge transfer resistance (R_{ct}) value.

Author Contributions: Conceptualization, S.W. and X.L.; methodology, S.W. and Z.P.; validation, T.Y., Z.P. and X.Y.; investigation, T.Y., Z.P. and X.Y.; data curation, Z.P. and X.Y.; writing—original draft preparation, Z.P. and S.W.; writing—review and editing, S.W. and X.L.; funding acquisition, S.W. All authors have read and agreed to the published version of the manuscript.

Funding: This work was supported by the National Natural Science Foundation of China (No. 52261019), and Major Discipline Academic and Technical Leaders Training Program of Jiangxi Province (No.20204BCJL23033).

Data Availability Statement: The data presented in this study are available in this article.

Conflicts of Interest: The authors declare no conflict of interest.

References

1. Williams, J.C.; Boyer, R.R. Opportunities and Issues in the Application of Titanium Alloys for Aerospace Components. *Metals* **2020**, *10*, 705. [CrossRef]
2. Dimitriu, S.; Dobrescu, M.; Vasilescu, M. Titanium and Titanium-Based Alloys for Aerospace. *Metal Int.* **2009**, *14*, 14–18.
3. Zhao, Q.; Sun, Q.; Xin, S.; Chen, Y.; Wu, C.; Wang, H.; Xu, J.; Wan, M.; Zeng, W.; Zhao, Y. High-strength Titanium Alloys for Aerospace Engineering Applications: A Review on Melting-forging Process. *Mater. Sci. Eng. A* **2022**, *845*, 143260. [CrossRef]

4. Jiang, X.P.; Man, C.S.; Shepard, M.J.; Zhai, T. Effects of Shot-Peening and Re-shot-peening on Four-Point Bend Fatigue Behavior of Ti-6Al-4V. *Mater. Sci. Eng. A* **2007**, *468–470*, 137–143. [CrossRef]
5. Xu, S.; Cao, Y.; Duan, B.; Liu, H.; Wang, J.; Si, C. Enhanced Strength and Sliding Wear Properties of Gas Nitrided Ti-6Al-4V Alloy by Ultrasonic Shot Peening Pretreatment. *Surf. Coat. Technol.* **2023**, *458*, 129325. [CrossRef]
6. Luo, X.; Dang, N.; Wang, X. The Effect of Laser Shock Peening, Shot Peening and Their Combination on the Microstructure and Fatigue Properties of Ti-6Al-4V Titanium alloy. *Int. J. Fatigue* **2021**, *103*, 106645. [CrossRef]
7. Gao, Y.K. Influence of Different Surface Modification Treatments on Surface Integrity and Fatigue Performance of TC4 Titanium Alloy. *Acta Metall. Sin.* **2016**, *52*, 915–922. (In Chinese)
8. Wen, M.; Liu, G.; Gu, J.F.; Guan, W.M.; Lu, J. The Tensile Properties of Titanium Processed by Surface Mechanical Attrition Treatment. *Surf. Coat. Technol.* **2008**, *202*, 4278–4733. [CrossRef]
9. Bozdana, A.T.; Gindy, N.N.Z.; Li, H. Deep Cold Rolling With Ultrasonic Vibrations-a New Mechanical Surface Enhancement Technique. *Int. J. Mach. Tool Manu.* **2005**, *45*, 713–718. [CrossRef]
10. Ao, N.; Liu, D.X.; Zhang, X.H.; Wu, S.C. Improved fretting fatigue mechanism of surface-strengthened Ti-6Al-4V alloy induced by ultrasonic surface rolling process. *Int. J. Fatigue* **2023**, *170*, 107567. [CrossRef]
11. Liu, C.S.; Liu, D.X.; Zhang, X.H.; Yu, S.M.; Zhao, W.D. Effects of the Ultrasonic Surface Rolling Process on the Fretting Fatigue Behavior of Ti-6Al-4V Alloy. *Materials* **2017**, *10*, 833. [CrossRef] [PubMed]
12. Tan, L.; Zhang, D.H.; Yao, C.F.; Ren, J.F. Effects of Ultrasonic Surface Rolling Parameters on Surface Integrity of TC17 Alloy. *J. Mater. Eng. Perform.* **2019**, *28*, 6736–6745. [CrossRef]
13. Ao, N.; Liu, D.X.; Zhang, X.H.; Liu, C.S.; Yang, J.; Liu, D. Surface Nanocrystallization of Body-Centered Cubic Beta Phase in Ti–6Al–4V Alloy Subjected to Ultrasonic Surface Rolling Process. *Surf. Coat. Technol.* **2019**, *361*, 35–41. [CrossRef]
14. Li, G.; Qu, S.G.; Pan, Y.X.; Li, X.Q. Effects of The Different Frequencies And Loads of Ultrasonic Surface Rolling on Surface Mechanical Properties and Fretting Wear Resistance of Hip Ti–6Al–4V Alloy. *Appl. Surf. Sci.* **2016**, *389*, 324–334. [CrossRef]
15. Pang, Z.W.; Wang, S.X.; Yin, X.L.; Yu, S.M.; Du, N. Effect of Spindle Speed during Ultrasonic Rolling on Surface Integrity and Fatigue Performance of Ti6Al4V Alloy. *Int. J. Fatigue* **2022**, *159*, 106794. [CrossRef]
16. Bozdana, A.T.; Gindy, N.N.Z. Comparative Experimental Study on Effects of Conventional and Ultrasonic Deep Cold Rolling Processes on Ti-6Al-4V. *Mater. Sci. Technol.* **2008**, *24*, 1378–1384. [CrossRef]
17. Li, G.; Qu, S.G.; Xie, M.X.; Ren, Z.J.; Li, X.G. Effect of Multi-Pass Ulstrasonic Surface Rolling on the Mechanical and Fatigue Properties of Hip Ti-6Al-4V Alloy. *Materials* **2017**, *10*, 133. [CrossRef]
18. Liu, C.S.; Liu, D.X.; Zhang, X.H.; He, G.Y.; Xu, X.C.; Ao, N.; Ma, A.M.; Liu, D. On the Influence of Ultrasonic Surface Rolling Process on Surface Integrity and Fatigue Performance of Ti-6Al-4V Alloy. *Surf. Coat. Technol.* **2019**, *370*, 24–34. [CrossRef]
19. Balusamy, T.; Kumar, S.; Sankara Narayanan, T.S.N. Effect of Surface Nanocrystallization on the Corrosion Behavior of AISI 409 Stainless Steel. *Corros. Sci.* **2010**, *52*, 3826–3834. [CrossRef]
20. Garbacz, H.; Pisarek, M.; Kurzydłowski, K.J. Corrosion Resistance of Nanostructured Titanium. *Biomol. Eng.* **2007**, *24*, 559–563. [CrossRef]
21. Waikar, R.A.; Guo, Y.B.; Liu, J.F.; Liu, Z.Y. Electrochemical Corrosion Behavior of Surface Nanocrystallized Steel and Aluminum Alloys by Air Blast Shot Peening (ABSP). In Proceedings of the 2016 International Symposium on Flexible Automation (ISFA), Cleveland, OH, USA, 1–3 August 2016; pp. 359–365. [CrossRef]
22. Xu, X.C.; Liu, D.X.; Zhang, X.H.; Liu, C.S.; Liu, D.; Ma, A.M. Effects of Ultrasonic Surface Rolling on the Localized Corrosion Behavior of 7B50-T7751 Aluminum Alloy. *Materials* **2020**, *13*, 738. [CrossRef] [PubMed]
23. Huang, H.W.; Wang, Z.B.; Liu, L.; Yong, X.P.; Lu, K. Formation of a Gradient Nanostructured Surface Layer on Martensitic Stainless Steel and Its Effect on Electrochemical Corrosion Behavior. *Acta Metal. Sin.* **2015**, *51*, 513–518.
24. Sun, Q.; Sun, J.; Han, J.; Wu, G. Corrosion Behavior in Hydrochloric Acid of Pure Titanium after Ultrasonic Severe Surface Rolling. *Metals* **2022**, *12*, 1951. [CrossRef]
25. Kumar, S.; Chattopadhyay, K.; Mahobia, G.S.; Singh, V. Hot Corrosion Behaviour of Ti–6Al–4V Modified by Ultrasonic Shot Peening. *Mater. Des.* **2016**, *110*, 196–206. [CrossRef]
26. Liu, C.S.; Liu, D.X.; Zhang, X.H.; Liu, D.; Ma, A.M.; Ao, N.; Xu, X.C. Improving Fatigue Performance of Ti-6Al-4V Alloy via Ultrasonic Surface Rolling Process. *J. Mat. Sci. Technol.* **2019**, *35*, 1555–1562. [CrossRef]
27. Ao, N.; Liu, D.X.; Xu, X.C.; Zhang, X.H.; Liu, D. Gradient Nanostructure Evolution and Phase Transformation of a Phase in Ti-6Al-4V Alloy Induced by Ultrasonic Surface Rolling Process. *Mater. Sci. Eng. A* **2019**, *742*, 820–834. [CrossRef]
28. Liu, D.; Liu, D.X.; Guagliano, M.; Xu, X.C.; Fan, K.F.; Bagherifard, S. Contribution of Ultrasonic Surface Rolling Process to the Fatigue Properties of TB8 Alloy with Body-Centered Cubic Structure. *J. Mater. Sci. Technol.* **2021**, *61*, 63–74. [CrossRef]
29. Wu, D.; Zheng, Y.; Wang, H.; Lv, H.; Liang, J.; Yu, J. Formation Mechanism of Nano-crystal on the Blade Surface Produced by Low-plasticity Ultrasonic Rolling Strengthening Process. *J. Manuf. Process.* **2023**, *90*, 357–376. [CrossRef]
30. Liu, D.; Liu, D.X.; Zhang, X.H.; Ma, A.M.; Liu, C.X. Microstructural Evolution Mechanisms in Rolled 17-4PH Steel Processed by Ultrasonic Surface Rolling Process. *Mater. Sci. Eng. A* **2020**, *773*, 138720. [CrossRef]
31. Xu, X.; Zhang, J.; Liu, H.; He, Y.; Zhao, W. Grain Refinement Mechanism under High Strain-Rate Deformation in Machined Surface during High Speed Machining Ti6Al4V. *Mater. Sci. Eng. A* **2019**, *752*, 167–179. [CrossRef]
32. Xu, Z.L.; Huang, C.W.; Wan, M.; Tan, C.S.; Zhao, Y.Q.; Ji, S.L.; Zeng, W.D. Influence of Microstructure on Strain Controlled Low Cycle Fatigue Crack Initiation and Propagation of Ti-55531 Alloy. *Int. J. Fatigue* **2022**, *156*, 10668. [CrossRef]

33. Hanlon, T.; Kwon, Y.N.; Suresh, S. Grain Size Effects on the Fatigue Response of Nanocrystalline Metals. *Scr. Mater.* **2003**, *49*, 675–680. [CrossRef]
34. Zhang, C.; Song, G.; Wang, Y.; Zheng, M.; Xiao, G.; Yang, J. Effect of Surface Nanocrystallization on Fatigue Crack Initiation and Propagation Behavior in Pure Zr. *Mater. Sci. Eng. A* **2020**, *794*, 139831. [CrossRef]
35. Guo, Y.B.; Warren, A.W.; Hashimoto, F. The Basic Relationships Between Residual Stress, White Layer, and Fatigue Life of Hard Turned and Ground Surfaces in Rolling Contact. *CIRP J. Manuf. Sci. Technol.* **2010**, *2*, 129–134. [CrossRef]
36. Luo, X.; Wang, Y.; Dang, N.; Tian, K.; Wang, K.; Zhao, C.; Zha, X.; Yu, Y. Gradient Microstructure and Foreign-object-damaged Fatigue Properties of Ti6Al4V Titanium Alloy Processed by the Laser Shock Peening and Subsequent Shot Peening. *Mater. Sci. Eng. A* **2022**, *849*, 143398. [CrossRef]
37. Assis, S.L.D.; Wolynec, S.; Costa, I. Corrosion Characterization of Titanium Alloys by Electrochemical Techniques. *Electrochim. Acta* **2006**, *51*, 1815–1819. [CrossRef]
38. Zhao, P.P.; Song, Y.W.; Dong, K.H.; Han, E.H. Synergistic Effect Mechanism of Different Ions on the Electrochemical Corrosion Behavior of TC4 Titanium Alloy. *Acta Metall. Sin.* **2023**, *59*, 939–946.
39. Orazem, M.E.; Tribollet, B. *Electrochemical Impedance Spectroscopy*, 1st ed.; Wiley, John & Sons: Hoboken, NJ, USA, 2008.
40. Wang, S.X.; Liu, X.H.; Wang, L.Q.; Wen, Q.J.; Du, N.; Huang, J.H. Formation Mechanism and Properties of Fluoride–Phosphate Conversion Coating on Titanium Alloy. *Rsc Adv.* **2017**, *7*, 16078–16086. [CrossRef]
41. Li, X.Q.; Wang, L.W.; Fan, L.; Zhong, M.Y.; Cheng, L.J.; Cui, Z.Y. Understanding the Effect of Fluoride on Corrosion Behavior of Pure Titanium in Different Acids. *Corros. Sci.* **2021**, *192*, 109812. [CrossRef]
42. Jelliti, S.; Richard, C.; Retraint, D.; Roland, T.; Chemkhi, M.; Demangel, C. Effect of Surface Nanocrystallization on the Corrosion Behavior of Ti–6Al–4V Titanium Alloy. *Surf. Coat. Technol.* **2013**, *224*, 82–87. [CrossRef]
43. Jin, L.; Cui, W.F.; Song, X.; Liu, G.; Zhou, L. Effects of Surface Nanocrystallization on Corrosion Resistance of β-Type Titanium Alloy. *Trans. Nonferrs. Met. Soc. China* **2014**, *24*, 2529–2535. [CrossRef]
44. Liu, X.; Ran, D.; Meng, H.M.; Li, Q.D.; Gong, X.F.; Long, B. Research Progress of the Effect of Surface Nanocrystallization on the Electrochemical Corrosion of Titanium Alloys. *Rare Met. Mater. Eng.* **2021**, *50*, 2244–2253.
45. Tang, J.; Luo, H.Y.; Zhang, Y.B. Enhancing the Surface Integrity and Corrosion Resistance of Ti-6Al-4V Titanium Alloy through Cryogenic Burnishing. *Int. J. Adv. Manuf. Technol.* **2017**, *88*, 2785–2793. [CrossRef]

Disclaimer/Publisher's Note: The statements, opinions and data contained in all publications are solely those of the individual author(s) and contributor(s) and not of MDPI and/or the editor(s). MDPI and/or the editor(s) disclaim responsibility for any injury to people or property resulting from any ideas, methods, instructions or products referred to in the content.